Statistical mechanical calculation of anisotropic step stiffness of a two-dimensional hexagonal lattice-gas model with next-nearest-neighbour interactions: application to Si(111) surface

1999 J. Phys.: Condens. Matter 11 6635

(http://iopscience.iop.org/0953-8984/11/35/302)

J. Phys.: Condens. Matter **11** (1999) 6635–6652. Printed in the UK PII: S0953-8984(99)02865-9

Statistical mechanical calculation of anisotropic step stiffness of a two-dimensional hexagonal lattice-gas model with next-nearest-neighbour interactions: application to Si(111) surface

Noriko Akutsu† and Yasuhiro Akutsu‡

† Faculty of Engineering, Osaka Electro-Communication University, Hatsu-cho, Neyagawa, Osaka 572, Japan
‡ Department of Physics, Graduate School of Science, Osaka University, Machikaneyama-cho, Toyonaka, Osaka 560, Japan

Received 22 March 1999, in final form 2 June 1999

Abstract. We study a two-dimensional honeycomb lattice-gas model with both nearest- and next-nearest-neighbour interactions in a staggered field, which describes the surface of a stoichiometrically binary crystal. We calculate the anisotropic step tension, step stiffness and equilibrium island shape, by an extended random walk method. We apply the results to the Si(111) 7×7 reconstructed surface and the high-temperature Si(111) 1×1 surface. We also calculate the inter-step interaction coefficient.

1. Introduction

Recent developments of experimental techniques such as STM (scanning–tunnelling microscopy) [1], LEEM (low-energy electron microscopy) [2] and REM (reflection electron microscopy) [3] make it possible to observe a step on a crystal surface in a wide range of length scales. However, the connection among quantities measured in different scales has not been clarified yet.

In [4], for a two-dimensional (2D) square-lattice Ising model with both nearest- and next-nearest-neighbour (nn and nnn) interactions, we calculated the anisotropic interface tension and interface stiffness by the imaginary path-weight (IPW) method which is an extended Feynman–Vdovichenko random walk method [5–8]. In the method, the overhang structure in a step is taken into account, which leads to high accuracy of the results in a wide range of temperature.

We applied the results to the Si(001) surface based on the microscopic kink energy obtained by Swartzentruber *et al* [9]. The Ising result gave a satisfactory explanation for experimentally measured step tension γ, step stiffness $\tilde{\gamma}$ and equilibrium island shape obtained by Bartelt *et al* [10] on the Si(001) surface.

In the present paper, we consider the honeycomb lattice Ising system in a staggered field, with both nn and nnn interactions, to calculate interface tension, interface stiffness, island shape and the coefficient of step interaction by the IPW method. We aim to apply the results to Si(111) 7×7 reconstructed surfaces and the high-temperature Si(111) 1×1 surface.

0953-8984/99/356635+18$30.00

2. Model Hamiltonian

We consider a honeycomb lattice with $2N$ sites. We decompose the lattice into two triangular sublattices designated by A and B. On the A sublattice, we define the occupation variable $C_{\mathrm{A}i}$ which takes 1 (present) or 0 (absent) at the site i. Similarly, we define $C_{\mathrm{B}j}$ for the B sublattice.

The lattice gas Hamiltonian $\mathcal{H}_{\mathrm{LG}}$ is then written as

$$\mathcal{H}_{\mathrm{LG}} = -4J_1 \sum_{\langle i,j\rangle}[C_{\mathrm{A}i}C_{\mathrm{B}j} - \tfrac{1}{2}(C_{\mathrm{A}i} + C_{\mathrm{B}j})] - 4J_{\mathrm{A2}} \sum_{\langle i,j\rangle}[C_{\mathrm{A}i}C_{\mathrm{A}j} - \tfrac{1}{2}(C_{\mathrm{A}i} + C_{\mathrm{A}j})]$$
$$-4J_{\mathrm{B2}} \sum_{\langle i,j\rangle}[C_{\mathrm{B}i}C_{\mathrm{B}j} - \tfrac{1}{2}(C_{\mathrm{B}i} + C_{\mathrm{B}j})] - \epsilon_{\mathrm{A}} \sum_{i=1}^{N} C_{\mathrm{A}i} - \epsilon_{\mathrm{B}} \sum_{i=1}^{N} C_{\mathrm{B}i} \tag{2.1}$$

where $4J_1$ is the bond energy between the A atom and B atom of the nn sites and $4J_{\mathrm{A2}}$ and $4J_{\mathrm{B2}}$ are the bond energies between nnn atoms. ϵ_{A} (ϵ_{B}) is the 'surface chemical potential' of the A atom (B atom). We consider the simplest case where ϵ_{A} and ϵ_{B} are given by

$$\left.\begin{aligned} \epsilon_{\mathrm{A}} &= \mu_{\mathrm{A,gas}}(P_{\mathrm{A}}, P_{\mathrm{B}}, T) - \mu_{\mathrm{A,surf}}(T) \\ \epsilon_{\mathrm{B}} &= \mu_{\mathrm{B,gas}}(P_{\mathrm{A}}, P_{\mathrm{B}}, T) - \mu_{\mathrm{B,surf}}(T) \end{aligned}\right\}. \tag{2.2}$$

In the above, $\mu_{\mathrm{A,gas}}(P_{\mathrm{A}}, P_{\mathrm{B}}, T)$ is the chemical potential of the A atom in the gas, P_{A} is the partial pressure of the A atom in the gas phase (similarly for $\mu_{\mathrm{B,solid}}(T)$, $\mu_{\mathrm{B,gas}}(P_{\mathrm{A}}, P_{\mathrm{B}}, T)$ and P_{B}); $\mu_{\mathrm{A,surf}}(T)$ and $\mu_{\mathrm{B,surf}}(T)$ are expressed as

$$\begin{aligned} \mu_{\mathrm{A,surf}} &= \Delta E(T) + \mu_{\mathrm{solid}}(T) \\ \mu_{\mathrm{B,surf}} &= -\Delta E(T) + \mu_{\mathrm{solid}}(T) \end{aligned} \tag{2.3}$$

where $\Delta E(T)$ has been introduced as the difference from the chemical potential of atoms in the bulk solid $\mu_{\mathrm{solid}}(T)$.

Let us consider the bulk phase-coexistence state of the stoichiometrically binary system. The total chemical potential of the system has to be unchanged under removal of one pair of AB atoms from crystal into vapour and vice versa. Hence, as the coexistence condition, we have

$$\mu_{\mathrm{A,gas}}(P_{\mathrm{A}}, P_{\mathrm{B}}, T) + \mu_{\mathrm{B,gas}}(P_{\mathrm{A}}, P_{\mathrm{B}}, T) = 2\mu_{\mathrm{solid}}(T). \tag{2.4}$$

Combining (2.2)–(2.4), we obtain

$$\epsilon_{\mathrm{B}} = -\epsilon_{\mathrm{A}}. \tag{2.5}$$

This condition also means that, in the lattice gas Hamiltonian (2.1), the total energy of the all-occupied state is the same at that of the all-empty state.

Let us introduce the Ising spin variables $\{\sigma_{\mathrm{A}i}\}$ and $\{\sigma_{\mathrm{B}i}\}$ as

$$\sigma_{\mathrm{A}i} = 2(C_{\mathrm{A}i} - \tfrac{1}{2}) \qquad \sigma_{\mathrm{B}i} = 2(\tfrac{1}{2} - C_{\mathrm{B}i}). \tag{2.6}$$

Substituting (2.6) into the Hamiltonian (2.1) together with (2.5), we have the Ising AF Hamiltonian $\mathcal{H}$:

$$\mathcal{H} = \mathcal{H}_{\mathrm{LG}} + Nz_6J_1 + Nz_3(J_{\mathrm{A2}} + J_{\mathrm{B2}})/2, = J_1 \sum_{\langle i,j\rangle} \sigma_{\mathrm{A}i}\sigma_{\mathrm{B}j} - J_{\mathrm{A2}} \sum_{\langle i,j\rangle} \sigma_{\mathrm{A}i}\sigma_{\mathrm{A}j} - J_{\mathrm{B2}} \sum_{\langle i,j\rangle} \sigma_{\mathrm{B}i}\sigma_{\mathrm{B}j}$$
$$-H \sum_{i=1}^{N} \sigma_{\mathrm{A}i} - H \sum_{i=1}^{N} \sigma_{\mathrm{B}i} + Nz_6J_1 + Nz_3(J_{\mathrm{A2}} + J_{\mathrm{B2}})/2 \qquad H = \epsilon_{\mathrm{A}}/2 \tag{2.7}$$

where $z_6 = 3$ and $z_3 = 6$ are the coordination numbers of honeycomb lattice and triangular lattice, respectively.

3. Imaginary path-weight method

We calculate interface quantities by a random walk method with imaginary path weight (IPW) [6–8]. We regard an interface with zigzag configuration as a trace of a 2D *free* random walk.

Consider an interface which connects sites O and P. We denote the distance between sites O and P by R (figure 1). The interface of the two-dimensional Ising model is made by fixing the boundary spins as depicted in figure 1. Let us denote the partition function the Ising model with and without interface by $Z_R^{+-}(\theta)$ and Z_R^{++}, respectively, where θ is the slant angle of an interface relative to a lattice axis [11, 12]. The interface tension $\gamma(\theta, T)$ is defined as

$$\gamma(\theta, T) = -k_B T \lim_{R\to\infty} \frac{1}{R} \ln\left[\frac{Z_R^{+-}(\theta)}{Z_R^{++}}\right] \tag{3.1}$$

where $Z_R^{+-}(\theta)/Z_R^{++}$ is regarded as the interface partition function $\mathcal{G}$.

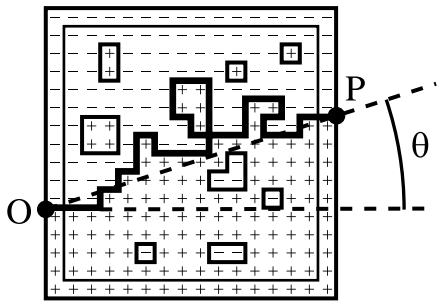

Figure 1. Examples of an interface of the square lattice Ising model made by fixing the boundary spins.

We apply Vdovichenko's method [5] to deal with the low-temperature diagrammatic expansion of $Z_R^{+-}(\theta)$ and Z_R^{++}. The method, which originally treated the high-temperature expansion of the partition function, also works for low-temperature expansion to evaluate the weighted sum over all possible domain-wall configurations. The essential point in the Vdovichenko method is the introduction of the imaginary factor $e^{i\phi/2}$ at each turn (with angle ϕ) of the random walks of the domain wall. With this simple recipe, the problem reduces to a free random walk problem on a lattice.

We see that Z_R^{++} equals the weighted sum over possible configurations of closed domain walls; and $Z_R^{+-}(\theta)$ equals the weighted sum over possible configurations of closed domain walls plus a single 'open' domain wall traversing the lattice. In evaluating $Z_R^{+-}(\theta)$ by Vdovichenko's method, the free random walk nature allows us to 'decouple' the open domain wall from closed domain walls [6, 7]. Therefore, in the limit of $R \to \infty$, the interface partition function is equivalent to the 'edge-to-edge' lattice Green function of the free random walk running on the dual lattice [7]. Thus, in the limit of $R \to \infty$, the interface partition function $\mathcal{G}$ is written as [7]

$$\mathcal{G} = \exp(-\gamma(\theta)R/k_B T) = \frac{1}{(2\pi)^2}\int_{-\pi}^{\pi}\int_{-\pi}^{\pi} dk_x\, dk_y \frac{e^{ikR}}{D(\boldsymbol{k})} \tag{3.2}$$

where the D-function is defined as

$$D(\boldsymbol{k}) = \det[1 - \hat{A}(\boldsymbol{k})]. \tag{3.3}$$

Here, $\hat{A}(\boldsymbol{k})$ is the Fourier component of the connectivity matrix $A(\boldsymbol{r})$ which characterizes the random walk.

The above-described imaginary path-weight random walk method to calculate $\gamma(\theta, T)$ is exact only for solvable cases. However, we have verified that the method works fairly well also for non-solvable cases [4, 8, 13, 14].

After evaluating the integral by the pure imaginary saddle point $\boldsymbol{\omega} = (\omega_x, \omega_y)$, we obtain a set of equations

$$\begin{aligned} &D(\mathrm{i}\boldsymbol{\omega}) = 0 \\ &\frac{\partial D(\mathrm{i}\boldsymbol{\omega})}{\partial \omega_y} \Big/ \frac{\partial D(\mathrm{i}\boldsymbol{\omega})}{\partial \omega_x} = \tan\theta \end{aligned} \tag{3.4}$$

and

$$\gamma(\theta, T) = k_{\mathrm{B}}T(\omega_x \cos\theta + \omega_y \sin\theta). \tag{3.5}$$

From the thermodynamical theory on equilibrium crystal shape (island shape) [16], we have,

$$\omega_x = \lambda y/k_{\mathrm{B}}T \qquad \omega_y = \lambda x/k_{\mathrm{B}}T \tag{3.6}$$

where λ is the Lagrange multiplier associated with the volume-fixing constraint in the Wulff construction, and x and y are the Cartesian coordinates describing the 2D island shape. Thus, we obtain the island shape directly from (3.4) with (3.5). Equation (3.6) gives relation between the interface orientation angle θ and the point (x, y) on the island shape.

The interface stiffness, which we denote by $\tilde{\gamma}(\theta)$, is given by [13]

$$\tilde{\gamma}(\theta) = \gamma(\theta) + \frac{\partial^2\gamma(\theta)}{\partial\theta^2} = k_{\mathrm{B}}T\sqrt{D_x^2 + D_y^2}[-D_{xx}\sin^2\theta + D_{xy}\sin 2\theta - D_{yy}\cos^2\theta]^{-1}, \tag{3.7}$$

where

$$D_x = \frac{\partial D}{\partial \omega_x} \qquad D_y = \frac{\partial D}{\partial \omega_x} \qquad D_{xx} = \frac{\partial^2 D}{\partial \omega_x^2} \qquad D_{yy} = \frac{\partial^2 D}{\partial \omega_y^2} \qquad D_{xy} = n\frac{\partial^2 D}{\partial \omega_x \omega_y}. \tag{3.8}$$

The one-dimensional interface of the lattice gas corresponds to a step on the vicinal surface. For the vicinal surfaces, the surface free energy per projected area, which we denote by $f(\rho)$, is written as [17–19]

$$f(\rho) = f(0) + \gamma(\theta)\rho + B(\theta)\rho^3 \qquad \rho = \frac{1}{a_h}\tan\phi \tag{3.9}$$

where ρ is the step density, ϕ is the tilted angle of the vicinal surface and a_h is the step height, and $B(\theta)$ is the inter-step interaction coefficient. We have [20, 21]

$$B(\theta) = \frac{\pi^2}{6}\frac{(k_{\mathrm{B}}T)^2}{\tilde{\gamma}(\theta)}\lambda^2(g_0) \qquad \lambda(g_0) = \frac{1}{2}\left(1 + \sqrt{1 + \frac{4\tilde{\gamma}(\theta)}{(k_{\mathrm{B}}T)^2}g_0}\right) \tag{3.10}$$

where g_0 is the coupling constant of the long-range interaction between the steps of the form g_0/r_s^2 (r_s is the step separation distance). Note that, in the limit of $g_0 \to 0$, the factor $\lambda(g)$ approaches unity, leading to [18, 19]

$$B(\theta) = \frac{\pi^2}{6}\frac{(k_{\mathrm{B}}T)^2}{\tilde{\gamma}(\theta)}. \tag{3.11}$$

Hence, the stiffness (3.7) can be utilized in determining the inter-step interaction coefficient $B(\theta)$.

4. The connectivity matrix and the D-function

4.1. The honeycomb lattice gas model with next-nearest-neighbour interaction

We apply the IPW method to calculate interface quantities of the nnn Ising model on the honeycomb lattice described by Hamiltonian (2.1), (2.7) (figure 2). The Fourier components of the connectivity matrix $(A_{m,n})$ are

$$
\begin{aligned}
A_{1,1} &= \exp(\mathrm{i}k_x)W/W_H \\
A_{2,1} &= \exp(\mathrm{i}k_x)W/W_H r_p \\
A_{3,1} &= \exp(\mathrm{i}k_x)W/W_H r_p r_p W_a \\
A_{5,1} &= \exp(\mathrm{i}k_x)W/W_H r_m r_m W_b \\
A_{6,1} &= \exp(\mathrm{i}k_x)W/W_H r_m \\
A_{1,2} &= \exp(\mathrm{i}k_x/2 + \mathrm{i}k_y c_y)W W_H r_m \\
A_{2,2} &= \exp(\mathrm{i}k_x/2 + \mathrm{i}k_y c_y)W W_H \\
A_{3,2} &= \exp(\mathrm{i}k_x/2 + \mathrm{i}k_y c_y)W W_H r_p \\
A_{4,2} &= \exp(\mathrm{i}k_x/2 + \mathrm{i}k_y c_y)W W_H r_p r_p W_b \\
A_{6,2} &= \exp(\mathrm{i}k_x/2 + \mathrm{i}k_y c_y)W W_H r_m r_m W_a \\
A_{1,3} &= \exp(-\mathrm{i}k_x/2 + \mathrm{i}k_y c_y)W/W_H r_m r_m W_b \\
A_{2,3} &= \exp(-\mathrm{i}k_x/2 + \mathrm{i}k_y c_y)W/W_H r_m \\
A_{3,3} &= \exp(-\mathrm{i}k_x/2 + \mathrm{i}k_y c_y)W/W_H \\
A_{4,3} &= \exp(-\mathrm{i}k_x/2 + \mathrm{i}k_y c_y)W/W_H r_p \\
A_{5,3} &= \exp(-\mathrm{i}k_x/2 + \mathrm{i}k_y c_y)W/W_H r_p r_p W_a \\
A_{2,4} &= \exp(-\mathrm{i}k_x)W W_H r_m r_m W_a \\
A_{3,4} &= \exp(-\mathrm{i}k_x)W W_H r_m \\
A_{4,4} &= \exp(-\mathrm{i}k_x)W W_H \\
A_{5,4} &= \exp(-\mathrm{i}k_x)W W_H r_p \\
A_{6,4} &= \exp(-\mathrm{i}k_x)W W_H r_p r_p W_b \\
A_{1,5} &= \exp(-\mathrm{i}k_x/2 - \mathrm{i}k_y c_y)W/W_H r_p r_p W_a \\
A_{3,5} &= \exp(-\mathrm{i}k_x/2 - \mathrm{i}k_y c_y)W/W_H r_m r_m W_b \\
A_{4,5} &= \exp(-\mathrm{i}k_x/2 - \mathrm{i}k_y c_y)W/W_H r_m \\
A_{5,5} &= \exp(-\mathrm{i}k_x/2 - \mathrm{i}k_y c_y)W/W_H \\
A_{6,5} &= \exp(-\mathrm{i}k_x/2 - \mathrm{i}k_y c_y)W/W_H r_p \\
A_{1,6} &= \exp(\mathrm{i}k_x/2 - \mathrm{i}k_y c_y)W W_H r_p \\
A_{2,6} &= \exp(\mathrm{i}k_x/2 - \mathrm{i}k_y c_y)W W_H r_p r_p W_b \\
A_{4,6} &= \exp(\mathrm{i}k_x/2 - \mathrm{i}k_y c_y)W W_H r_m r_m W_a \\
A_{5,6} &= \exp(\mathrm{i}k_x/2 - \mathrm{i}k_y c_y)W W_H r_m \\
A_{6,6} &= \exp(\mathrm{i}k_x/2 - \mathrm{i}k_y c_y)W W_H \\
\text{others} &= 0
\end{aligned}
\tag{4.1}
$$

where $\mathrm{i}^2 = -1$, $c_y = \sqrt{3}/2$, $W = \exp[-2(J_1 + 2J_{A2} + 2J_{B2})/(k_B T)]$, $W_H = \exp[-2H/(3k_B T)]$, $W_a = \exp[4J_{A2}/(k_B T)]$, $W_b = \exp[4J_{B2}/(k_B T)]$, $r_p = \exp(\mathrm{i}\pi/6)$ and $r_m = \exp(-\mathrm{i}\pi/6)$.

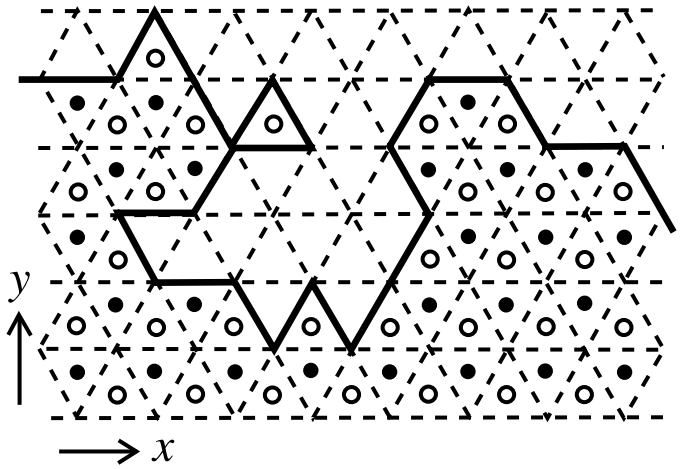

Figure 2. Examples of an interface configuration. A atom and B atom are indicated by filled circle and open circle, respectively. The thick line represents an interface.

Then, the D-function defined by (3.3) is

$$\begin{aligned}D(k_x,k_y) = {} & M + c_1\cosh(k_x) + c_1\cosh(k_x/2 - c_yk_y) + c_1\cosh(k_x/2 + c_yk_y) + c_2\cosh(2k_x)\\ & + c_2\cosh(k_x - 2c_yk_y) + c_2\cosh(k_x + 2c_yk_y) + c_3\cosh(2c_yk_y)\\ & + c_3\cosh(3k_x/2 - c_yk_y) + c_3\cosh(3k_x/2 + c_yk_y) + s_1\sinh(k_x) + s_2\sinh(2k_x)\\ & - s_2\sinh(k_x - 2c_yk_y) + s_4\sinh(k_x/2 - c_yk_y) + s_4\sinh(k_x/2 + c_yk_y)\\ & - s_2\sinh(k_x + 2c_yk_y)\end{aligned} \tag{4.2}$$

where

$$\begin{aligned}M = {} & 1 + 3W^2 + 4W^6 - W^3/W_H^3 - W^3W_H^3 - 12W^6W_a + 9W^6W_a^2 + 4W^6W_a^3\\ & + (W^3W_a^3)/W_H^3 + W^3W_H^3W_a^3 - 6W^6W_a^4 + W^6W_a^6 - 12W^6W_b\\ & + 30W^6W_aW_b + (3W^3W_aW_b)/W_H^3 + 3W^3W_H^3W_aW_b - 18W^6W_a^2W_b\\ & - 6W^6W_a^3W_b + 6W^6W_a^4W_b + 9W^6W_b^2 - 18W^6W_aW_b^2 + 3W^4W_a^2W_b^2\\ & + 9W^6W_a^2W_b^2 + 4W^6W_b^3 + (W^3W_b^3)/W_H^3 + W^3W_H^3W_b^3 - 6W^6W_aW_b^3\\ & + 2W^6W_a^3W_b^3 - 6W^6W_b^4 + 6W^6W_aW_b^4 + W^6W_b^6\end{aligned} \tag{4.3}$$

$$\begin{aligned}c_1 = {} & W^2/W_H^2 - W^4/W_H^2 - W/W_H - WW_H + W^2W_H^2 - W^4W_H^2 + (W^4W_a)/W_H^2\\ & + W^4W_H^2W_a + (W^4W_a^2)/W_H^2 + W^4W_H^2W_a^2 - (W^4W_a^3)/W_H^2 - W^4W_H^2W_a^3\\ & + (W^4W_b)/W_H^2 + W^4W_H^2W_b - (W^2W_aW_b)/W_H^2 - (W^4W_aW_b)/W_H^2\\ & + (2W^3W_aW_b)/W_H - (2W^5W_aW_b)/W_H + 2W^3W_HW_aW_b\\ & - 2W^5W_HW_aW_b - W^2W_H^2W_aW_b - W^4W_H^2W_aW_b + (3W^5W_a^2W_b)/W_H\\ & + 3W^5W_HW_a^2W_b - (W^5W_a^4W_b)/W_H - W^5W_HW_a^4W_b + (W^4W_b^2)/W_H^2\\ & + W^4W_H^2W_b^2 + (3W^5W_aW_b^2)/W_H + 3W^5W_HW_aW_b^2 - (3W^5W_a^2W_b^2)/W_H\\ & - 3W^5W_HW_a^2W_b^2 - (W^4W_b^3)/W_H^2 - W^4W_H^2W_b^3 - (W^5W_aW_b^4)/W_H\\ & - W^5W_HW_aW_b^4\end{aligned} \tag{4.4}$$

$$c_2 = [W^3(1 + W_H^2)(-1 + W_a)(-1 + W_b)]/W_H \tag{4.5}$$

$$c_3 = 2W^4(-1 + W_a)(-1 + W_b)(-1 + W_a + W_b + W_aW_b) \tag{4.6}$$

$$\begin{aligned}s_1 = -[&W(-1+W_H)(1+W_H)(W - W^3 + W_H + WW_H^2 - W^3W_H^2 + W^3W_a + W^3W_H^2W_a\\ &+W^3W_a^2 + W^3W_H^2W_a^2 - W^3W_a^3 - W^3W_H^2W_a^3 + W^3W_b + W^3W_H^2W_b\\ &-WW_aW_b - W^3W_aW_b - 2W^2W_HW_aW_b + 2W^4W_HW_aW_b - WW_H^2W_aW_b\\ &-W^3W_H^2W_aW_b - 3W^4W_HW_a^2W_b + W^4W_HW_a^4W_b + W^3W_b^2 + W^3W_H^2W_b^2\\ &-3W^4W_HW_aW_b^2 + 3W^4W_HW_a^2W_b^2 - W^3W_b^3 - W^3W_H^2W_b^3\\ &+W^4W_HW_aW_b^4)]/W_H^2 \end{aligned} \tag{4.7}$$

$$s_2 = -[W^3(-1+W_H)(1+W_H)(-1+W_a)(-1+W_b)]/W_H \tag{4.8}$$

$$\begin{aligned}s_4 = [&W(-1+W_H)(1+W_H)(W - W^3 + W_H + WW_H^2 - W^3W_H^2 + W^3W_a + W^3W_H^2W_a\\ &+W^3W_a^2 + W^3W_H^2W_a^2 - W^3W_a^3 - W^3W_H^2W_a^3 + W^3W_b + W^3W_H^2W_b\\ &-WW_aW_b - W^3W_aW_b - 2W^2W_HW_aW_b + 2W^4W_HW_aW_b - WW_H^2W_aW_b\\ &-W^3W_H^2W_aW_b - 3W^4W_HW_a^2W_b + W^4W_HW_a^4W_b + W^3W_b^2 + W^3W_H^2W_b^2\\ &-3W^4W_HW_aW_b^2 + 3W^4W_HW_a^2W_b^2 - W^3W_b^3 - W^3W_H^2W_b^3\\ &+W^4W_HW_aW_b^4)]/W_H^2. \end{aligned} \tag{4.9}$$

We substitute the D-function into (3.4) and solve with respect to (ω_x, ω_y) as a function of θ. Substituting the solution $(\omega_x(\theta), \omega_y(\theta))$ into (3.5)–(3.8), we obtain the interface tension, 2D island shape and the interface stiffness.

Note that the D-function has mirror symmetry with respect to k_x-axis, i.e. $D(k_x, k_y) = D(k_x, -k_y)$. Therefore, the island shape has mirror symmetry with respect to the k_x-axis. That is, $\omega_y(0) = 0$ and $\omega_y(\pi) = 0$ are the solutions of (3.4). At the orientation corresponding to $\theta = 0$ or $\theta = \pi$, the form (4.2) reduces to

$$\begin{aligned}D(k_x, 0) = M &+ c_3 + c_1\cosh(k_x) + 2c_1\cosh(k_x/2) + c_2\cosh(2k_x) + 2c_2\cosh(k_x)\\ &+2c_3\cosh(3k_x/2) + s_1\sinh(k_x) + s_2\sinh(2k_x) - 2s_2\sinh(k_x)\\ &+2s_4\sinh(k_x/2). \end{aligned} \tag{4.10}$$

From the solution of $D(k_x, 0) = 0$ ($\omega_y(0) = \omega_y(\pi) = 0$), we obtain $\cosh(\omega_x(0)/2)$ and $\cosh(\omega_x(\pi)/2)$. Then, from (3.5), step tension becomes

$$\gamma(0) = 2k_BT\cosh^{-1}(\omega_x(0)/2) \qquad \gamma(\pi) = 2k_BT\cosh^{-1}(\omega_x(\pi)/2). \tag{4.11}$$

In the $T \to 0$ limit, step tension (step free energy per lattice constant) becomes

$$\begin{aligned}\gamma(0) &= \min[2J_1 + 4J_2 + \tfrac{2}{3}H, 2(2J_1 + 4J_2 - \tfrac{2}{3}H)]\\ \gamma(\pi) &= \min[2J_1 + 4J_2 - \tfrac{2}{3}H, 2(2J_1 + 4J_2 + \tfrac{2}{3}H)]\end{aligned} \tag{4.12}$$

where $\min[a, b]$ denotes the smaller one in $\{a, b\}$.

From (3.7), the step stiffness becomes

$$\begin{aligned}\tilde{\gamma}(0) = k_BT[&|c_1\sinh(\omega_x(0)/2) + (c_1 + 2c_2)\sinh(\omega_x(0)) + 3c_3\sinh(3\omega_x(0)/2)\\ &+2c_2\sinh(2\omega_x(0)) + s_4\cosh(\omega_x(0)/2) + (s_1 + 2s_2)\cosh(\omega_x(0))\\ &+2s_2\cosh(2\omega_x(0))|]/[2c_y^2(2c_3 + c_1\cosh(\omega_x(0)/2) + 4c_2\cosh(\omega_x(0))\\ &+c_3\cosh(3\omega_x(0)/2) + s_4\sinh(\omega_x(0)/2) - 4s_2\sinh(\omega_x(0)))] \end{aligned} \tag{4.13}$$

$$\begin{aligned}\tilde{\gamma}(\pi) = k_BT[&|c_1\sinh(\omega_x(\pi)/2) + (c_1 + 2c_2)\sinh(\omega_x(\pi)) + 3c_3\sinh(3\omega_x(\pi)/2)\\ &+2c_2\sinh(2\omega_x(\pi)) + s_4\cosh(\omega_x(\pi)/2) + (s_1 + 2s_2)\cosh(\omega_x(\pi))\\ &+2s_2\cosh(2\omega_x(\pi))|]/[2c_y^2(2c_3 + c_1\cosh(\omega_x(\pi)/2) + 4c_2\cosh(\omega_x(\pi))\\ &+c_3\cosh(3\omega_x(\pi)/2) + s_4\sinh(\omega_x(\pi)/2) - 4s_2\sinh(\omega_x(\pi)))]. \end{aligned} \tag{4.14}$$

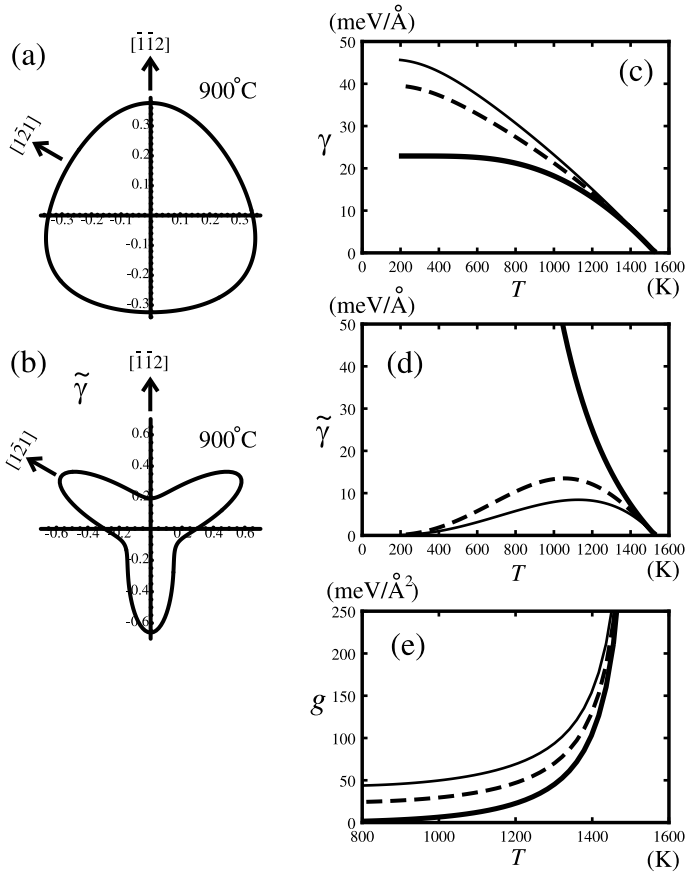

Figure 3. An example of calculation by the use of the D-function of (4.2). (a) The island shape at 900 °C, (b) a polar graph of step stiffness at 900 °C, (c) temperature dependence of step tension, (d) temperature dependence of step stiffness and (e) temperature dependence of $g = B/a_h^3$. We have set $J_1 = 165$ meV, $J_2 = -16.5$ meV and $H = 165$ meV. Kink energies are 88 meV for the $(2\bar{1}\bar{1})$ step and 176 meV for the $(\bar{2}11)$ step. In (c)–(e), thick lines correspond to $(\bar{2}11)$ steps, thin lines to $(2\bar{1}\bar{1})$ steps and broken lines to $\{10\bar{1}\}$ steps.

In figure 3, we show an example of an equilibrium island shape and a polar graph of step stiffness at $J_1 = 165$ meV, $J_2/J_1 = -0.1$, lattice constant = 3.84 Å and $H/J_1 = 1$. We also show the temperature dependence of step tension, step stiffness, the coefficient of step interaction (3.11) where $g = B/a_h^3$, $a_h = 3.14$ Å and $g_0 = 0$.

In the absence of nnn interactions, W_a and W_b reduce to unity. The D-function (4.2), then, becomes

$$D(k_x, k_y) = M + c_1\cosh(k_x) + 2c_1\cosh(k_x/2 - c_yk_y) + c_1\cosh(k_x/2 + c_yk_y) + s_1\sinh(k_x) + s_4\sinh(k_x/2 - c_yk_y) + s_4\sinh(k_x/2 + c_yk_y) \tag{4.15}$$

$$M = 1 + 3W^2 + 3W^4 + W^6 + 4W^3(W_H^3 + 1/W_H^3)$$
$$c_1 = -(1-W)^2W(1+W)^2(1+W_H^2)/W_H$$
$$s_1 = -s_4 = (1-W)^2W(1+W)^2(1+W_H)(1-W_H)/W_H \qquad c_2 = c_3 = s_2 = 0 \tag{4.16}$$

which agrees with the D-function given in [13].

4.2. The case of $H = 0$

At $H = 0$, s_1, s_2 and s_4 in (4.2) become zero, since W_H reduces to unity. The D-function, then, has the symmetry $D(k_x, k_y) = D(\pm k_x, \pm k_y)$. The island shape has mirror symmetry with respect to the k_y-axis too; $\omega_x(\pi/2) = \omega_x(3\pi/2) = 0$ becomes the solution of (3.4). The equation

$$D(0, k_y) = M + c_1 + c_2 + 2(c_1 + c_3)\cosh(c_y k_y) + (2c_2 + c_3)\cosh(2c_y k_y) = 0 \tag{4.17}$$

is solved, in terms of $\cosh(c_y\omega_y)$ ($k_y = \mathrm{i}\omega_y$), as

$$\cosh(c_y\omega_y) = -\frac{c_1 + c_3}{2(2c_2 + c_3)} + \sqrt{\frac{(c_1 + c_3)^2}{4(2c_2 + c_3)^2} + \frac{-c_1 + c_2 + c_3 - M}{2(2c_2 + c_3)}} \equiv z. \tag{4.18}$$

By use of this solution, we obtain the step tension as

$$\gamma(\pi/2) = \gamma(3\pi/2) = \frac{k_B T}{c_y}\cosh^{-1}(z) \tag{4.19}$$

and the step stiffness as

$$\tilde{\gamma}(\pi/2) = \tilde{\gamma}(3\pi/2) = \frac{-4k_B T c_y\sqrt{z^2 - 1}|c_1 + c_3 + 2(2c_2 + c_3)z|}{2c_1 + 4c_2 + (c_1 + 9c_3)z + 8c_2 z^2}. \tag{4.20}$$

In the case of $J_{A2} = J_{B2} = 0$, the D-function reduces to that of the exact solution for the nn honeycomb lattice system [22].

That is,

$$\begin{aligned} &D(k_x, k_y) = M + c_1\cosh(k_x) + c_1\cosh(k_x/2 - c_y k_y) + c_1\cosh(k_x/2 + c_y k_y) \\ &M = (1 + W)^2(1 - 2W + 6W^2 - 2W^3 + W^4) \\ &c_1 = -2(1 - W)^2 W(1 + W)^2 \qquad c_2 = c_3 = s_1 = s_2 = s_4 = 0. \end{aligned} \tag{4.21}$$

At $\theta = 0$, we obtain an explicit form of the solutions as

$$\omega_y(0) = 0 \qquad \cosh(\omega_x(0)/2) = \tfrac{1}{2}\sqrt{3 - 2M/c_1} - \tfrac{1}{2}. \tag{4.22}$$

Also, at $\theta = \pi/2$, we have

$$\omega_x(\pi/2) = 0 \qquad \cosh(c_y\omega_y(\pi/2)) = \tfrac{1}{2}(-M/c_1 - 1). \tag{4.23}$$

Hence, the interface tensions become

$$\begin{aligned} &\gamma(0) = 2k_B T\ln(m_y) \\ &m_y = -\tfrac{1}{2} + \tfrac{1}{2}z_2 + \tfrac{1}{2}\sqrt{(z_2 - 3)(z_2 + 1)} \\ &z_2 = \frac{(1 + W)\sqrt{1 - W + W^2}}{\sqrt{W}|1 - W|} \end{aligned} \tag{4.24}$$

$$\gamma(\pi/2) = 1/c_y k_B T\ln[(-2 + 1/W + W)/2]. \tag{4.25}$$

Due to the Wulff theorem, $\gamma(0)$ and $\gamma(\pi/2)$ give the linear size of the island shape along x- and y-directions. The explicit form of interface stiffness becomes

$$\tilde{\gamma}(0) = \frac{k_B T}{c_y^2}\frac{z_2\sqrt{-3 - 2z_2 + z_2}}{2(z_2 - 1)} \tag{4.26}$$

$$\tilde{\gamma}(\pi/2) = 4k_B T c_y\frac{(1 + W^2)|1 - 4W + W^2|}{1 + 4W - 6W^2 + 4W^3 + W^4}. \tag{4.27}$$

4.3. Triangular lattice

In the limit of $J_1 \to 0$, the system becomes two independent triangular lattice gases. In this case, the random walk treatment on the honeycomb lattice may not be good enough. In fact, (4.2) in this limit gives a D-function slightly different from the known exact one on the triangular lattice. Hence, we need a separate study to treat this case.

The D-function of the triangular lattice becomes

$$D_3(k_x, k_y) = M - c_1 \cosh(k_y) - c_2 \cosh(\sqrt{3}k_x/2 - k_y/2) - c_3 \cosh(\sqrt{3}k_x/2 + k_y/2), \tag{4.28}$$

where

$$M = 1 + W_1^2W_2^2 + W_1^2W_3^2 + W_2^2W_3^2 \qquad c_1 = 2(1 - W_1)(1 + W_1)W_2W_3$$
$$c_2 = 2W_1W_2(1 - W_3)(1 + W_3) \qquad c_3 = 2W_1(1 - W_2)(1 + W_2)W_3 \tag{4.29}$$

$W_1 = \exp[-2J_1/(k_BT)]$, $W_2 = \exp[-2J_2/(k_BT)]$ and $W_3 = \exp[-2J_3/(k_BT)]$. The equations agree with the known exact one [22]. Note that the form of $D_3(k_x, k_y)$ (4.27) is essentially the same as $D(k_x, k_y)$ of the nn honeycomb lattice (4.20). Therefore, the island shape of the triangular lattice obtained from (3.4) is the same as the one of the honeycomb lattice. The difference is the temperature dependence of coefficients. When $J_1 = J_2 = J_3 = J$, i.e. $W_1 = W_2 = W_3 = W$, the D-function has a symmetry of $D_3(k_x, k_y) = D_3(\pm k_x, \pm k_y)$. Hence, we have explicit forms of γ and $\tilde{\gamma}$ for special orientations. Therefore, we have

$$\gamma_3(0) = \frac{2}{\sqrt{3}}k_BT \ln\left[\frac{1 - W^2}{2W^2}\right] \tag{4.30}$$

$$\gamma_3(\pi/2) = 2k_BT\cosh^{-1}\left(-\frac{1}{2} + \frac{1}{2}\sqrt{3 + \frac{1 + 3W^4}{W^2(1 - W)(1 + W)}}\right). \tag{4.31}$$

The step stiffness is written as

$$\tilde{\gamma}_3(0) = \frac{2\sqrt{3}k_BT(1 + W^2)|1 - 3W^2|}{1 + 6W^2 - 3W^4} \tag{4.32}$$

$$\tilde{\gamma}_3(\pi/2) = \frac{2k_BT}{3}\frac{\sqrt{(1 + 3W^2)(1 + 3W^4 - 2Wz_1 + 2W^3z_1)}}{W(z_1 - W)|1 - W^2|} \qquad z_1 = \sqrt{\frac{1 + 3W^2}{1 - W^2}}. \tag{4.33}$$

5. Application to Si(111) surface

5.1. The 7 × 7 reconstructed surface

At temperatures lower than the $7 \times 7 \leftrightarrow 1 \times 1$ transition temperature ($\sim$1130 K), the Si(111) surface forms a 7×7 reconstructed structure called the DAS (dimer adatom stacking-fault) structure [23]. The unit cell of the DAS structure is divided into the faulted half (FH) and the unfaulted half (UH) [24], each of which forms a triangular lattice. It has been observed that the step structure is well described by the combination of the FH unit and UH unit [25]. We consider, therefore, a pair of triangular sublattices, where the one represents the FH lattice system, and the other represents the UH one. Consequently, the system becomes equivalent to a stoichiometrically binary lattice gas on a honeycomb lattice with nn interactions, where the inequivalent sites of the lattice gas model are coarse-grained representations of these two halves of the 7×7 unit cell. Therefore, we can use (4.15) and (4.16) to calculate step quantities. In figure 2, we regard closed circles as FH units, and open circles as UH units. We set lattice

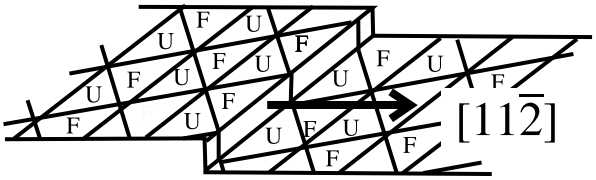

Figure 4. Examples of a step edge on the 7×7 reconstructed Si(111) surface. 'U' denotes an unfaulted half unit, and 'F' denotes a faulted half unit.

constant $= 3.84 \times 7$ Å and step height $= 3.14$ Å. We introduce the step running direction angle θ so that a straight step with $\theta = 0$ corresponds to the $(11\bar{2})$ step (figure 4).

In spite of the extensive experimental studies on Si(111)7×7 structure, the values of kink energy and step tension have not been settled yet. As one trial, we adopt the result of Eaglesham *et al* [26] where step tension γ at 700 °C was obtained from the equilibrium crystal shape (ECS) of Si: $\gamma_{111} = 5.7 \times 10^{-11}$ J m^{-1} for the (111) surface and $\gamma_{100} = 1.0 \times 10^{-11}$ J m^{-1} for the (100) surface. Due to the 2×1 reconstruction, this value of γ_{100} corresponds to the mean value of the S_A-step tension and the S_B-step tension, and is consistent with the one calculated in our previous papers [4, 15].

We choose kink energy so that the calculated mean value of step tension for $(2\bar{1}\bar{1})$ and $(\bar{2}11)$ at 700 °C reproduces the above mentioned value 5.7×10^{-11} J m^{-1} ($= 36$ meV Å^{-1}). In addition, the experimental observation of the island shape (and also the shape of the spiral step) gives further information on the kink energy, due to the Wulff theorem for 2D ECS. Let h_n be the distance between the centre (= Wulff point) of the ECS (island shape, in our case) and the tangential line of the ECS at a position on the ECS curve, where $\boldsymbol{n}$ is the interface normal vector at the position. The Wulff theorem states that the ratio h_n/γ_n (γ_n: interface tension, or step tension in our case) is $\boldsymbol{n}$ independent, leading to a relation $\gamma_n/\gamma_{n'} = h_n/h_{n'}$ for arbitrary $\boldsymbol{n}$ and $\boldsymbol{n}'$. From the photographs of the experimental observation [27, 28], we have $h_{\bar{2}11}/h_{2\bar{1}\bar{1}} = 1.2$. This ratio gives the ratio between the step free energies corresponding to these directions. At the low temperature where the observation was made, these step free energies are well approximated by the step formation energies $(2J + 2H/3)$ and $(2J - 2H/3)$ (see (4.12)), giving us $h_{\bar{2}11}/h_{2\bar{1}\bar{1}} = 1.2 = (2J + 2H/3)/(2J - 2H/3)$ which amounts to $H/J = 0.31$.

We then set $J = 0.475$ eV and $H = 0.15$ eV. The kink energy becomes 1.05 eV $= 2J + 2H/3$ for the $(2\bar{1}\bar{1})$ step and 0.85 eV $= 2J - 2H/3$ for the $(\bar{2}11)$ step, which are smaller than but of the same order as magnitude of the ones reported in [29] and [21].

The difference in the on-site energy between the UH and FH, is then $E_{FH} - E_{UH} = 4H = 0.59$ eV. In the first principles study of Meade and Vanderbilt [30], surface energies of the Si(111) surface for various structures are calculated: for example, 1.24 eV/1×1 for the 2×2-adatom structure, and 1.27 eV/1×1 for the 2×2-adatom (faulted) structure. From these values, we can estimate $E_{FH} - E_{UH}$ to be $(1.27 - 1.24) \times 24 \sim 0.7$ eV which is in reasonable agreement with our value 0.59 eV.

In figure 5, we show equilibrium island shape at 400 °C and 850 °C, and the temperature dependence of step tension, step stiffness and step interaction coefficient $g = B/a_h^3$ (see (3.11)). The step tension is almost constant below 1130 K, because the temperature is very low as compared with the lattice-gas melting temperature of the model (∼8300 K). On the other hand, the step stiffness strongly depends on temperature in the same region. The step stiffness for the $(2\bar{1}\bar{1})$ step increases rapidly as temperature decreases, while the step stiffness of the $(0\bar{1}1)$ step becomes smaller and smaller and converges to zero at zero temperature.

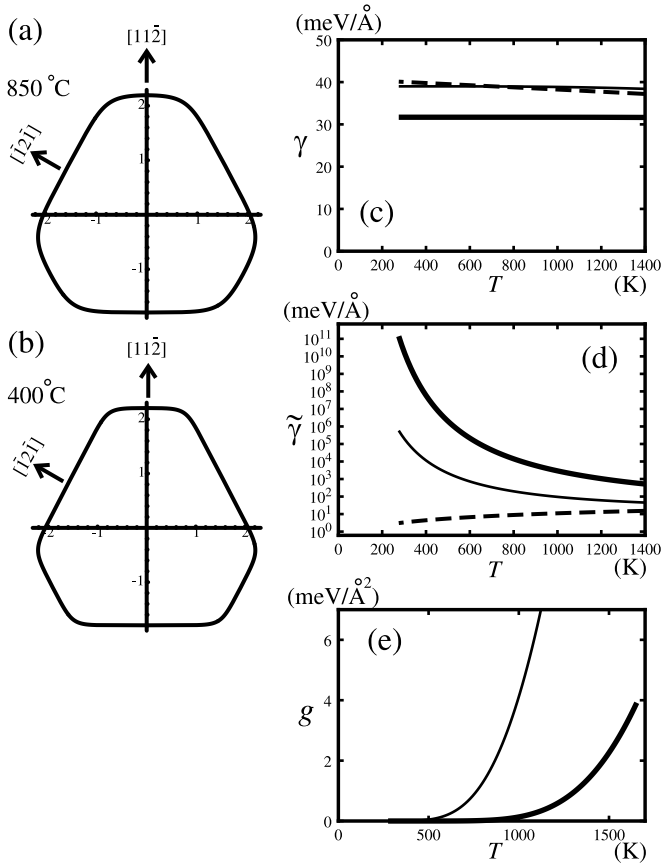

Figure 5. Calculation for 7×7 reconstructed surface by the use of the D-function of (4.15). (a) The island shape at 850 °C, (b) the island shape at 400 °C, (c) temperature dependence of step tension, (d) temperature dependence of step stiffness and (e) temperature dependence of $g = B/a_h^3$. We have set $J = 0.475$ eV, $4H = 0.59$ eV. Kink energy $= 1.05$ eV for the $(2\bar{1}\bar{1})$ step and 0.85 eV for the $(\bar{2}11)$ step. In (c)–(e), thick lines correspond to $(2\bar{1}\bar{1})$ steps, thin lines to $(\bar{2}11)$ steps and broken lines to $\{10\bar{1}\}$ steps.

Note that a similar analysis can be made for an $n\times n$ DAS structure. From the photographs of a small island of 5×5 structure [28], we find that the island shape has a sixfold rotational symmetry in contrast to the case of the 7×7 structure which has a threefold rotational symmetry. Recall that the sixfold rotational symmetry appears only when $H = 0$ (see section 4.2). Therefore, the energy difference between FH and UH units in the case of the 5×5 DAS structure is very small if it exists. We stress here that, also for other structures, observation of the anisotropy of the equilibrium island shape will be useful in determining the energy difference between FH and UH units.

5.2. The 1 × 1 high-temperature surface

The high-temperature Si(111) surface at about 900 °C has the structure of the 1×1 surface together with disordered adatoms with concentration of 0.25 [31–33]. Further, Kohmoto and Ichimiya [31] reported that the number ratio of adatoms sitting on the T_4 site and H_3 site is 4:1. Although the adatoms are considered to be in a disordered phase, broad $\sqrt{3}\times\sqrt{3}$ peaks

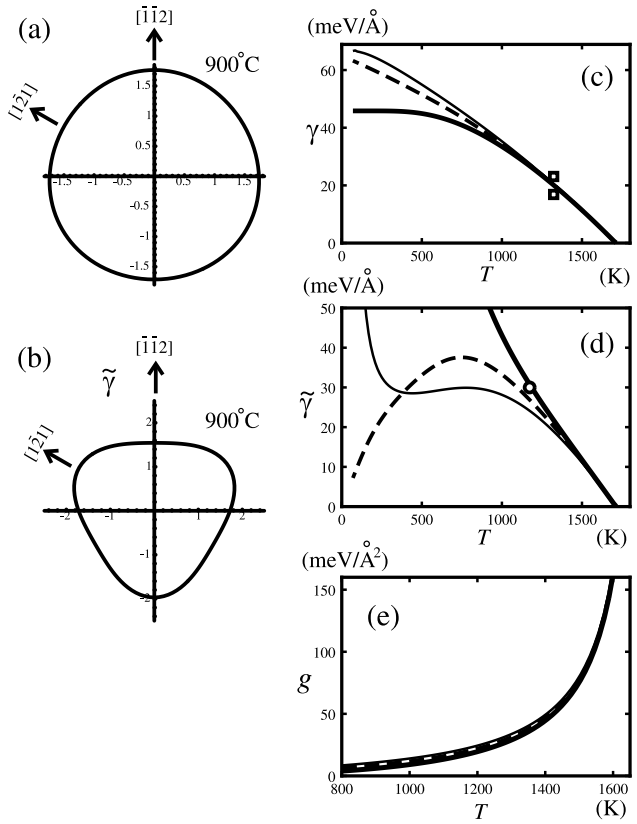

Figure 6. Calculation for 1×1 surface (case 1) by the use of D-function of (4.2). (a) The island shape at 900 °C, (b) a polar graph of step stiffness at 900 °C, (c) temperature dependence of step tension, (d) temperature dependence of step stiffness and (e) temperature dependence of $g = B/a_h^3$. We have set $J_1 = 60$ meV, $J_2 = 12$ meV and $H = 60$ meV. Kink energy = 176 meV for the $(2\bar{1}\bar{1})$ step and 256 meV for the $(\bar{2}11)$ step. In (c)–(e), thick lines correspond to $(2\bar{1}\bar{1})$ steps, thin lines to $(\bar{2}11)$ steps and broken lines to $\{10\bar{1}\}$ steps. Open squares: [38]. Open circle: [36].

appear in diffraction observations [31, 34] which suggests the existence of short-range order corresponding to formation of the hard-hexagon units [35].

For the high-temperature surface of Si(111), experimental measurement of the step tension and the step stiffness has been a subject of active study [21, 36–39]. The experimental values are, however, not settled yet. We make, therefore, several trial calculations for possible cases. In all cases, we choose the microscopic coupling constants so that the calculated step stiffness at 900 °C reproduces the value presented by Bartelt *et al* [36].

5.2.1. Case 1: adatom in disordered phase without short-range order. We use the honeycomb lattice-gas system of (4.2), with J_1 and J_2 being regarded as effective coupling constants.

In figure 2 we regard the filled circles as atoms of the top layer and the open circles as those of the second layer (the lattice constant = 3.84 Å, the step height $a_h = 3.14$ Å).

We introduce the step running direction angle θ so that a straight step with $\theta = 0$ corresponds to the $(\bar{1}\bar{1}2)$ step. The effect of dangling bonds normal to the (111) plane are taken into account by setting $H/J_1 = 1$.

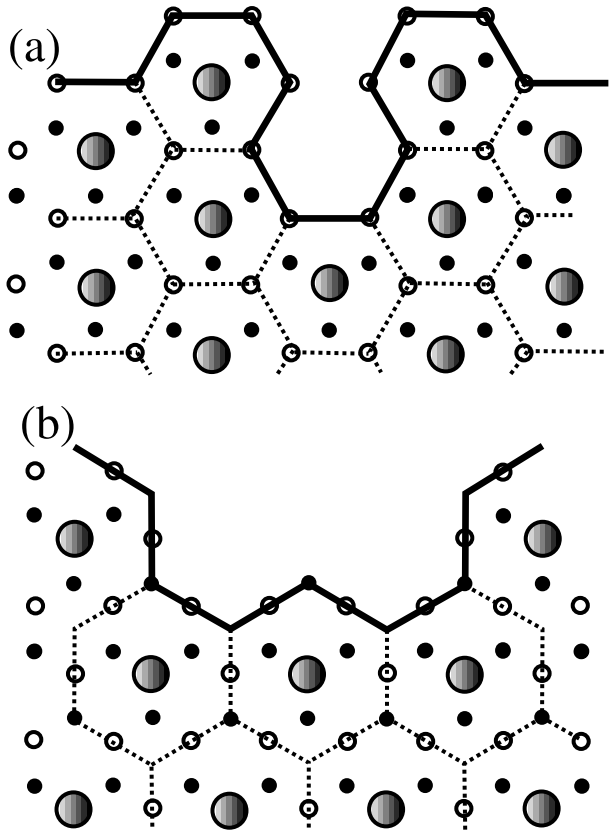

Figure 7. Examples of an interface configuration for two cases of adatom orderings: (a) $\sqrt{3} \times \sqrt{3}$ and (b) 2×2. The thick line represents the interface. A atoms and B atoms are indicated by filled circles and open circles, respectively. Adatoms are indicated by shaded large circles. Broken lines denote boundaries between the hexagons.

We calculate equilibrium island shape, step stiffness and step interaction coefficient, which we show in figure 6. Here, assuming that J_2 is small, we have set $J_2/J_1 = 0.2$ and $J_1 = 60$ meV. The kink energy becomes 176 meV for the $(2\bar{1}\bar{1})$ step and 256 meV for the $(\bar{2}11)$ step. As is seen in the island shape and the polar graph of step stiffness at 900 °C, there remains anisotropy in the step stiffness in spite of the circular island shape. The most significant characteristic of this result is the asymmetry between the orientations $(2\bar{1}\bar{1})$ and $(\bar{2}11)$. In contrast to the 7×7 structure, the stiffness as a function of the step orientation takes its maximum at $(\bar{2}11)$.

5.2.2. Case 2: the $\sqrt{3} \times \sqrt{3}$ short-range ordered phase. In the case of the $\sqrt{3} \times \sqrt{3}$ ordered phase of adatoms, we calculate step quantities by using the triangular lattice-gas model (figure 7(a)). As has been pointed out in section 4, the system has sixfold rotational symmetry. We set the lattice constant to be $3.84 \times \sqrt{3}$ Å, and the step height to be 3.14 Å. We introduce

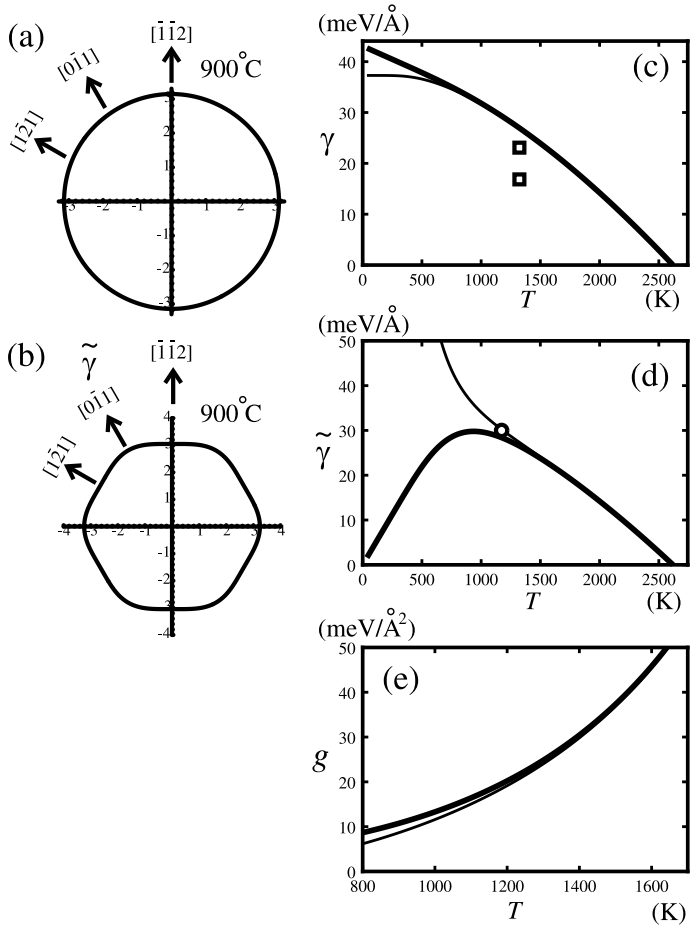

Figure 8. Case 2. Calculation for $\sqrt{3} \times \sqrt{3}$ adatom ordering (case 2) by the use of the D-function of (4.30)–(4.33). (a) The island shape at 900 °C, (b) a polar graph of step stiffness at 900 °C, (c) temperature dependence of step tension, (d) temperature dependence of step stiffness, (e) temperature dependence of $g = B/a_h^3$. We have set $J = 62$ meV. Kink energy = 248 meV for the $\{10\bar{1}\}$ step. In (c)–(e), thick lines correspond to $\{2\bar{1}\bar{1}\}$ steps and thin lines to $\{10\bar{1}\}$ steps. Open squares: [38]. The open circle: [36].

the step running direction angle θ so that a straight step with $\theta = 0$ corresponds to the $(\bar{1}\bar{1}2)$ step. The step tension and the step stiffness are calculated exactly from (4.30)–(4.33). The effective coupling constant is obtained to be $J = 62$ meV (kink energy = 248 meV). We show the calculated results in figure 8. The step stiffness takes its maximum at the orientation $\{10\bar{1}\}$.

5.2.3. Case 3: the 2 × 2 short-range ordered phase. Calculation of step quantities can be done in the same fashion as in case 2. We set the lattice constant as 3.84 × 2 Å, and the step height as 3.14 Å (figure 7(b)). We introduce the step running direction angle θ so that a straight step with $\theta = 0$ corresponds to $(0\bar{1}1)$ step. The step stiffness takes its maximum at $\{\bar{2}11\}$. The effective coupling constant is obtained to be $J = 67$ meV (kink energy = 268 meV). We show the calculated results in figure 9.

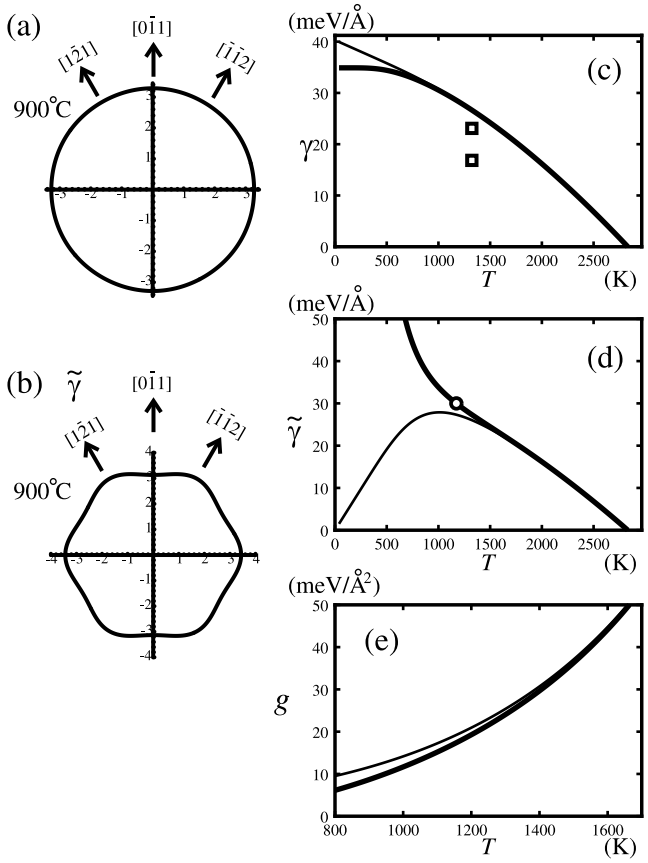

Figure 9. Case 3. Calculation for 2×2 adatom ordering (case 3) by the use of the D-function of (4.30)–(4.33). (a) The island shape at 900 °C, (b) a polar graph of step stiffness at 900 °C, (c) temperature dependence of step tension, (d) temperature dependence of step stiffness and (e) temperature dependence of $g = B/a_h^3$. We have set $J = 67$ meV: Kink energy = 268 meV for the $2\bar{1}\bar{1}$ step. In (c)–(e), thick lines correspond to $\{2\bar{1}\bar{1}\}$ steps and thin lines to $\{10\bar{1}\}$ steps. Open squares: [38]. The open circle: [36].

6. Summary

We have considered the honeycomb lattice Ising system in a staggered field with both nearest-neighbour (nn) and next-nearest-neighbour (nnn) interactions, to calculate interface tension, interface stiffness and island shape by the imaginary path-weight (IPW) method.

We have applied the calculated results to Si(111) 7×7-reconstructed surfaces and the high-temperature Si(111) 1×1 surface. We have made an estimation of the microscopic coupling constants from existing experimental data, and have drawn the equilibrium island shape, step tension, step stiffness and the coefficient of step interaction, with their temperature dependence. Our analysis made in the present paper will be helpful in determining precise value of the kink energy from experimental observation.

Our lattice-gas treatment made in the present paper corresponds to the two-level approximation for the surface fluctuation. Fortunately, the temperature range of our concern in the present study is very low: the two-level approximation is expected to be fairly reliable.

On the other hand, at higher temperatures, near the roughening transition temperature, we should consider multilevel fluctuation of the surface. Even in such cases, we have an efficient method, namely, the *temperature-rescaled Ising-model approach* [15], where the IPW method is combined with the numerical renormalization-group method [40]; details will be discussed elsewhere.

Acknowledgments

The authors thank Professor T Yasue, Professor E D Williams, Professor A Ichimiya, Dr T Suzuki and Professor H Iwasaki for helpful discussions. One of the authors (NA) thanks Professor T Yasue for bibliographical information. The authors also thank Professor T Nishinaga for encouragement. This work was partially supported by the 'Research for the Future' Programme from the Japan Society for the Promotion of Science (JSPS-RFTF97P00201) and by a Grant-in-Aid for Scientific Research from the Ministry of Education, Science, Sports and Culture (No 09640462).

References

[1] Binnig G, Rohrer H, Gerber Ch and Weibel E 1983 *Phys. Rev. Lett.* **49** 120
[2] Bauer E 1985 *Ultramicroscopy* **17** 57
Bauer E and Telieps W 1987 *Scanning Micros. Suppl.* **1** 99
Bauer E and Telieps W 1988 *The Study of Surfaces and Interfaces by Electon Optical Techniques* ed A Howie and U Valderé (New York: Plenum) p 195
[3] Yagi K 1987 *J. Appl. Cryst.* **20** 147
Inoue N, Tanishiro Y and Yagi K 1987 *Japan. J. Appl. Phys.* **26** L293
Nakayama T, Tanishiro Y and Takayanagi K 1987 *Japan. J. Appl. Phys.* **26** L1186
[4] Akutsu N and Akutsu Y 1997 *Surf. Sci.* **376** 92
[5] Vdovichenko N V 1964 *Zh. Eksp. Teor. Fiz.* **47** 715 (Engl. trans. 1965 *Sov. Phys.–JETP* **20** 477)
Feynman R P 1972 *Statistical Mechanics* (Reading, MA: Benjamin–Cummings)
[6] Holzer M 1990 *Phys. Rev. Lett.* **64** 653
Holzer M 1990 *Phys. Rev.* B **42** 10 570
[7] Akutsu Y and Akutsu N 1990 *Phys. Rev. Lett.* **64** 1189
[8] Akutsu N and Akutsu Y 1990 *J. Phys. Soc. Japan* **59** 3041
[9] Swartzentruber B S, Mo Y-W, Kariotis R, Lagally M G and Webb M B 1990 *Phys. Rev. Lett.* **65** 1913
Swartzentruber B S and Schacht M 1995 *Surf. Sci.* **322** 83
[10] Bartelt N C, Tromp R M and Williams E D 1994 *Phys. Rev. Lett.* **73** 1656
[11] Zia R K P 1978 *Phys. Lett.* A **64** 345
[12] Abraham D B 1986 *Phase Transitions and Critical Phenomena* vol 10, ed C Domb and J L Lebowitz (New York: Academic) p 1
[13] Akutsu N 1992 *J. Phys. Soc. Japan* **61** 477
[14] Akutsu N and Akutsu Y 1995 *J. Phys. Soc. Japan* **64** 736
[15] Akutsu N and Akutsu Y 1998 *Phys. Rev.* B **57** R4233
[16] Andreev A F 1981 *Zh. Eksp. Teor. Fiz.* **80** 2042 (Engl. trans. 1982 *Sov. Phys.–JETP* **53** 1063)
[17] Gruber E E and Mullins W W 1967 *J. Phys. Chem. Solids* **28** 6549
Pokrovsky V L and Talapov A L 1979 *Phys. Rev. Lett.* **42** 65 (Engl. trans. 1980 *Sov. Phys.–JETP* **51** 134)
[18] Akustu Y, Akutsu N and Yamamoto T 1988 *Phys. Rev. Lett.* **61** 424
[19] Yamamoto T, Akutsu Y and Akutsu N 1988 *J. Phys. Soc. Japan* **57** 453
[20] Yamamoto T, Akutsu Y and Akutsu N 1994 *J. Phys. Soc. Japan* **63** 915
[21] Williams E D, Phaneuf R J, Wei J, Bartelt N C and Einstein T L 1993 *Surf. Sci.* **294** 219
Williams E D, Phaneuf R J, Wei J, Bartelt N C and Einstein T L 1994 *Surf. Sci.* **310** 451
[22] Zia R K P 1986 *J. Stat. Phys.* **45** 801
[23] Takayanagi K, Tanishiro Y, Takahashi S and Takahashi M 1985 *J. Vac. Sci. Technol.* A **3** 1502
[24] Neddermeyer H 1996 *Rep. Prog. Phys.* **59** 701
[25] Tochihara H, Shimada W, Itoh M, Tanaka H, Udagawa M and Sumita I 1992 *Phys. Rev.* B **45** 11332
Miki K, Morita Y, Tokumoto H, Sato T, Iwatsuki M, Suzuki M and Fukuda T 1992 *Ultramicroscopy* **42**–**44** 851

[26] Eaglesham D J, White A E, Feldman L D, Moriya N and Jacobson D C 1993 *Phys. Rev. Lett.* **70** 1643
[27] Yagi K, Yamanaka K, Sato H, Shima M, Ohse H, Ozawa S and Tanishiro Y 1991 *Prog. Theor. Phys. Suppl.* **106** 303
[28] Ichimiya A, Nakahara H and Tanaka Y 1996 *Thin solid Films* **281**/**282** 1
Ichimiya A, Nakahara H and Tanaka Y 1996 *J. Cryst. Growth* **163** 39
[29] Wilhelmi G, Kampschulte T and Neddermeyer H 1995 *Surf. Sci.* **331**–**333** 1408
[30] Meade R D and Vanderbilt D 1989 *Phys. Rev.* B **40** 3905
[31] Kohmoto S and Ichimiya A 1989 *Surf. Sci.* **223** 400
[32] Latyshev A V, Krasilnikov A B, Aseev A L, Sokolov L V and Stenin S I 1991 *Surf. Sci.* **254** 90
[33] Yang Y-N and Williams E D 1994 *Phys. Rev. Lett.* **72** 1862
[34] Ino S 1977 *Japan. J. Appl. Phys.* **16** 891
Iwasaki H, Hasegawa S, Akizumi M, Li S-Te, Nakamura S and Kanamori J 1987 *J. Phys. Soc. Japan* **56** 3425
[35] Sakamoto Y and Kanamori J 1989 *J. Phys. Soc. Japan* **58** 2083
[36] Bartelt N C, Goldberg J L, Einstein T L, Williams E D, Heyraud J C and Métois J J 1993 *Phys. Rev.* B **48** 15 453
[37] Alfonso C, Heyraud J C and Métois J J 1993 *Surf. Sci.* **291** L745
Bermond J M, Métois J J, Heyraud J C and Alfonso C 1995 *Surf. Sci.* **331**–**333** 855
[38] Bermond M, Métois J J, Egea X and Floret F 1995 *Surf. Sci.* **330** 48
Suzuki T, Métois J J and Yagi K 1995 *Surf. Sci.* **339** 105
[39] Latyshev A V, Minoda H, Tanishiro H and Yagi K 1996 *Phys. Rev. Lett.* **76** 94
Latyshev A B, Aseev A L, Krasilnikov A B and Stenin S I 1989 *Surf. Sci.* **213** 157
Métois J J and Audiffren M 1997 *Int. J. Mod. Phys.* B **11** 3691
[40] White S R 1992 *Phys. Rev. Lett.* **69** 2863
Nishino T 1995 *J. Phys. Soc. Japan* **64** 3598
Nishino T and Okunishi K 1995 *J. Phys. Soc. Japan* **64** 4084